Egypt.J.Chem. **Vol. 62**, No. 12, pp. 2213 - 2228 (2019)

Egyptian Journal of Chemistry
http://ejchem.journals.ekb.eg/

P_2O_5– F- U Characterization and Depositional Environment of Phosphatic Rocks for the Duwi Formation, Qussier- Safaga Region, Red Sea Coast, Egypt

Esmat A. Abou El-Anwar, Hamed S. Mekky* and Wael Abdel Wahab
Geological Sciences Department, National Research Centre, 33 El-Buhous Street,

THE Duwi Formation in Qusseir-Safaga region is conformably overlain by the Qusseir variegated shales and underlain by the Dakhla shales. The studied phosphatic rocks in the Duwi Formation, is an attractive rock unit for it's enrichment in heavy metals and U content.

Mineralogically, phosphatic rocks in the Duwi Formation are mainly composed mainly of fluorapatite, in addition to minor occurrence of calcite, dolomite, gypsum, quartz, and pyrite. Geochemical data reveal that the rocks of the Duwi Formation were deposited under anoxic environments. The present study used the statistical result of the interrelation between P_2O_5, F and U concentrations on Egyptian phosphate samples and compared to the measured data. Uranium mostly occurs in an oxidized U^{6+} state. It could be fixed with the phosphatic ion, forming secondary uranium phosphate minerals such as phosphuranylite and belovite in Qusseir region. In addition to Uranyl phosphates, uranium minerals in Safaga region contain also Uranyl carbonates and Uranyl sulfates, which had been attributed to the post-depositional U enrichment. The chemical data and index show that the phosphatic rocks in Safaga region are more enriched in the majority trace and rare earth elements, and are subjected to high chemical weathering than those in Qusseir region.

Keywords: Qusseir-Safaga, Duwi Phosphates, Fluorapatite, Trace Elements, Phosphuranylite.

Introduction

Type and source are the most important factors control the mineralogical composition of the phosphate rocks. They are classified into four groups. Sedimentary marine origin (75%), igneous source (15-20%), metamorphic and weathered rocks (8%), and 2-3% as biogenic sources. Silica, clayey and calcareous materials are gangue minerals for the sedimentary phosphate origin.

The most sedimentary calcareous phosphate rocks have been significant quantities of carbonates and are considered as carbonate-apatite or francolites. Phosphorites contain more than 18 -20% P_2O_5 as a sedimentary source. Most phosphorites are of marine origin. Francolite (carbonate-flourapatite) is the main phosphate mineral.

In 2007 quadratic regression model was theoretically developed with widely used in many practices, after one year, in 2008, geochemists statistically applied it on phosphate ores and recognized the U concentration in mg/kg base on two predictor variables X1, X2 that represent P_2O_5 and F concentrations in wt.%; respectively. Rock phosphate deposits contain many million tonnes of uranium, which may be extracted as a by-product of making fertilisers. The presence of uranium in marine phosphorus generally explains either calcium replacement in the structure of apatite mineral or the absorption of uranium in mixed organic matter and encoded apatite [1].

The phosphatic rocks are mainly consisted of authigenic peloids and bioclasts. Peloids are

*Corresponding author e-mail: mekkyhamed60@gmail.com
Received 1/4/2019; Accepted 17/6/2019
DOI: 10.21608/ejchem.2019.11366.1728

considered as authigenic or reworked in origin [2,3]. The formation of phosphorites may be carried nutrients from deep water into the photic zone [4], formed in situ [5] or fluvial input [6].

The word today depends on phosphate rocks as a source of phosphorous (P) fertilizer to enhance soil productivity in addition nitrogen (N) and potassium (K) fertilizer in modern farming.

Physical and chemical pathways include processes that do not prevail in deep-sea environments and in fact do not often coincide in space and time even on continental margins, contributing to the scarcity of high quality phosphoric deposits and reduction of phosphate rock reserves [7].

The present work will study the mineralogical and geochemical characteristics of the phosphate rocks in Yunis (Qusseir) and Um El-Hwutat (Safaga) mines of the Duwi Formation at Qusseir-Safaga region, in an effort to recognize its depositional environment and the economic evolution.

Geological Setting

The sedimentary phosphatic rocks (Upper Cretaceous - Eocene) are originated in marine environments [7]. In Egypt, the phosphatic rocks of Duwi Formation are located in the Nile Valley, the Red Sea Coast, Abu Tartur plateau and Sinai. The Duwi Formation in the Qusseir-Safaga region is conformably overlain by the Qusseir variegated shales and underlain by the Dakhla shales [8]. Duwi Formation in Egypt represents the early stage of the Late Cretaceous marine transgression. It was classified into four members according to its lithology [9]. The most of the phosphate beds appear as massive rocks. Their thickness up to tens of centimeters.

The chosen area is represented by Yunis and Um El-Hwutat mines (Fig. 1). They are occurring at the upper member of Duwi Formation in Qusseir-Safaga region (Fig. 2). Phosphatic rocks in Yunis mines are formed as horizontal layers, which extend into their tunnels to several kilometers. These phosphatic beds are deposited above a layer of the black shales. They are varies in thickness, which are increase downwards. In some places of these mines, the thickness of phosphatic ore decreases is related to the black shales. Yunis mines represented a huge stockpile of phosphate that is still under threat. The chosen area in Yunis mines is located at longitudes 34^0 03 ′12″- 34^0 03 ′24 ″E and Latitudes 26^O 11 ′27″ - 26^O 11 ′37 ″N which is located south of the Hamrawin mines, 12 km from Qusseir - Safag Asflt Roada to west (Fig. 1 and 2), [9].

Um El-Hwutat mines, about 7 km from a residential village named the Um El-Hwutat. This village has a big mosque and an enormous number of houses. Um El-Hwutat mines have several openings, some of them are close together and the other is separated.

The mines have traces of a railway line and tunnels extended to several kilometers. Phosphatic rocks in these mines extend horizontally to tens of kilometers, and range in thickness from tens of centimeters to extra meters. This layer of phosphate is confined between two-layers of the black shales. The lower layer extends along to the phosphatic bed. This layer of the black shales is homogeneous and ranges in color from light gray to dark black. Whereas the black shales overlies are ranges in color from green to yellow, and the red color resulting of it contains iron oxides. This succession is caped with calcareous limestones. Um El-Hwutat mines is located at Longitudes 34^0 11′ 23″- 34^0 11 ′33 ″E and Latitudes 26^O 03 ′01″ - 26^O 03 ′13 ″N (Fig. 1 and 2), [9].

Sampling and Methodology

Twenty representative samples were collected from the phsophatic rocks from Yunis and Um El-Hwutat mines. Mineralogically, selected four samples were investigated by the X-ray technique at using a PANalytical X-Ray Diffraction equipment model X′Pert PRO with Secondary Monochromator, Cu- radiation (λ=1.542Å) at 45 K.V., 35 M.A. and scanning speed 0.02^o/sec. The morphology and the size of the synthesized samples were characterized via SEM coupled with energy-dispersive spectroscopy EDX, (SEM Model Quanta FEG 250). Ten samples were selected to determine the chemical composition by using Axios Sequential WD-XRF Spectrometer, PANalytical 2005 in the National Research Center laboratories. ASTM E 1621 standard guide for elemental analysis by wavelength dispersive X-Ray Fluorescence Spectrometer, and ASTM D 7348 standard test methods for loss of ignition (LOI) of solid Combustion.

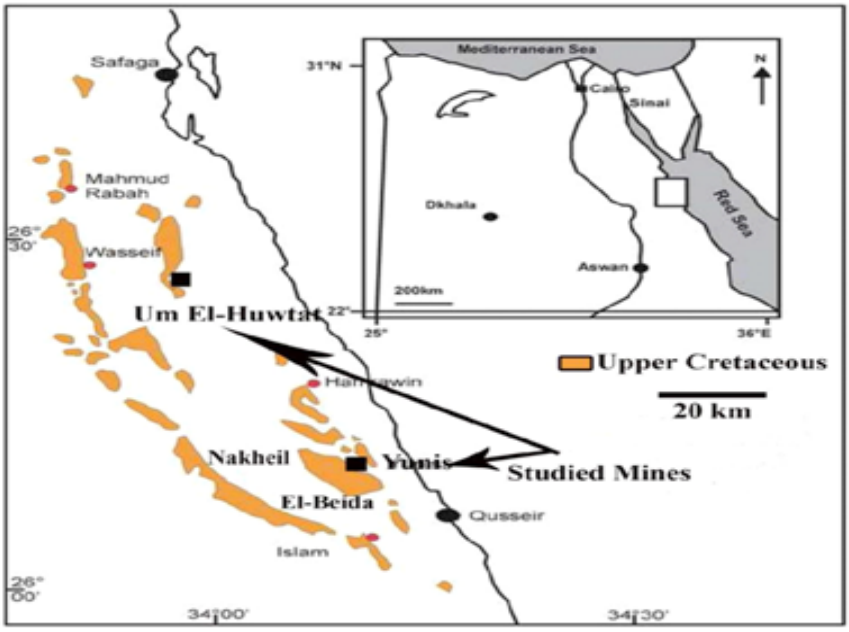

Fig. 1. The location map of the studied mines.

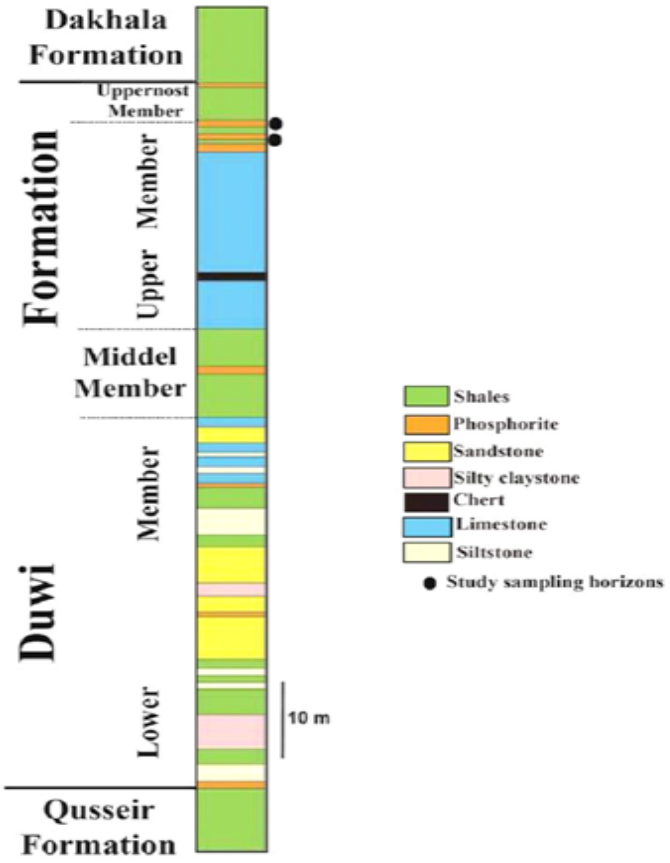

Fig. 2. Stratigraphic columnar section of the Duwi Formation in the Red Sea region (after Baioumy and Tada, 2005).

Results and Discussion

Mineralogy

The mineralogical composition, that identified by using the X-Ray technique, showed six mineral phases in the studied sedimentary rocks of Duwi phosphorites. Apatite (fluor-apatite) is the dominance (Fig. 3), which conformed to SEM. Apatite (francolites) reveals that the phosphatic rocks contain significant quantities of carbonates. In addition to Apatite, there were five non-phosphatic minerals; quartz, calcite, gypsum, dolomite and pyrite.

SEM and EDX examination of the phosphatic samples show the dominance bone fragments (Fig. 4), EDX recorded P (12.78%) and Ca (30.75%). Framboidal pyrite as authigenic origin are scattered in the matrix (Fig. 5). Framboidal pyrite is dispersed in irregular masses and clusters, which suggesting anoxic conditions during the early diageneting stages [10- 14]. Pyrite as spheres may be a mark indicating shallow marine water [15]. During the weathering, pyrite could be oxidized and changes to ferruginous materials that indicate the role of chemical weathering. Thus, the Duwi Formation seems to be significantly affected by chemical weathering, which is in agreement with [13, 14, 16].

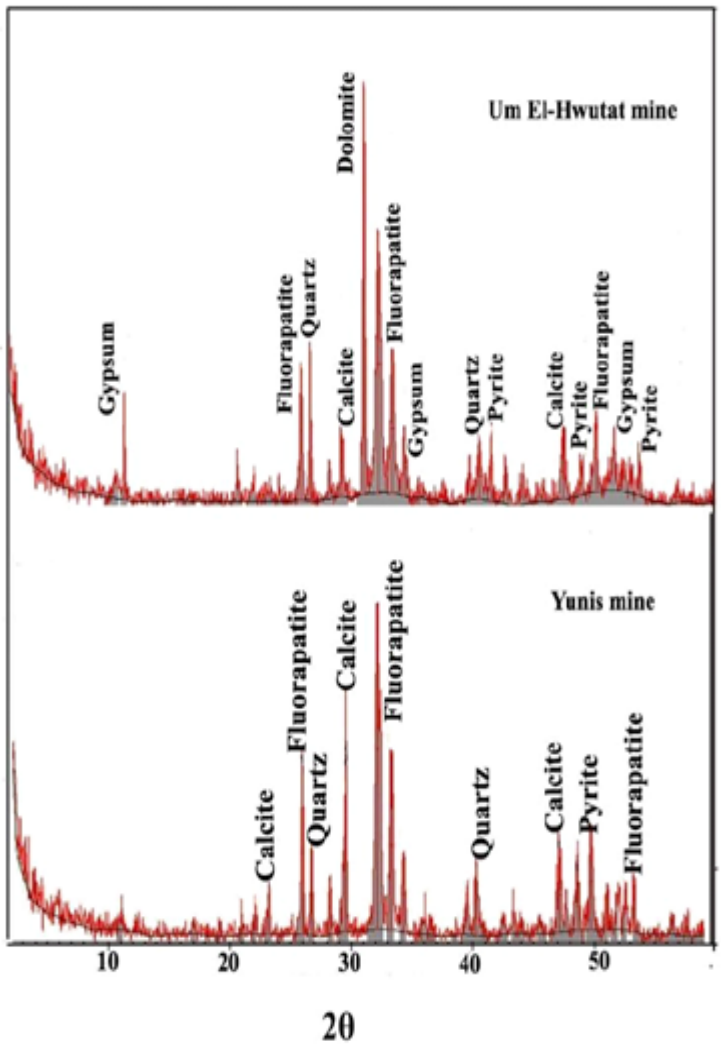

Fig. 3. X-Ray diffractograms for the phosphatic rocks of the studied mines.

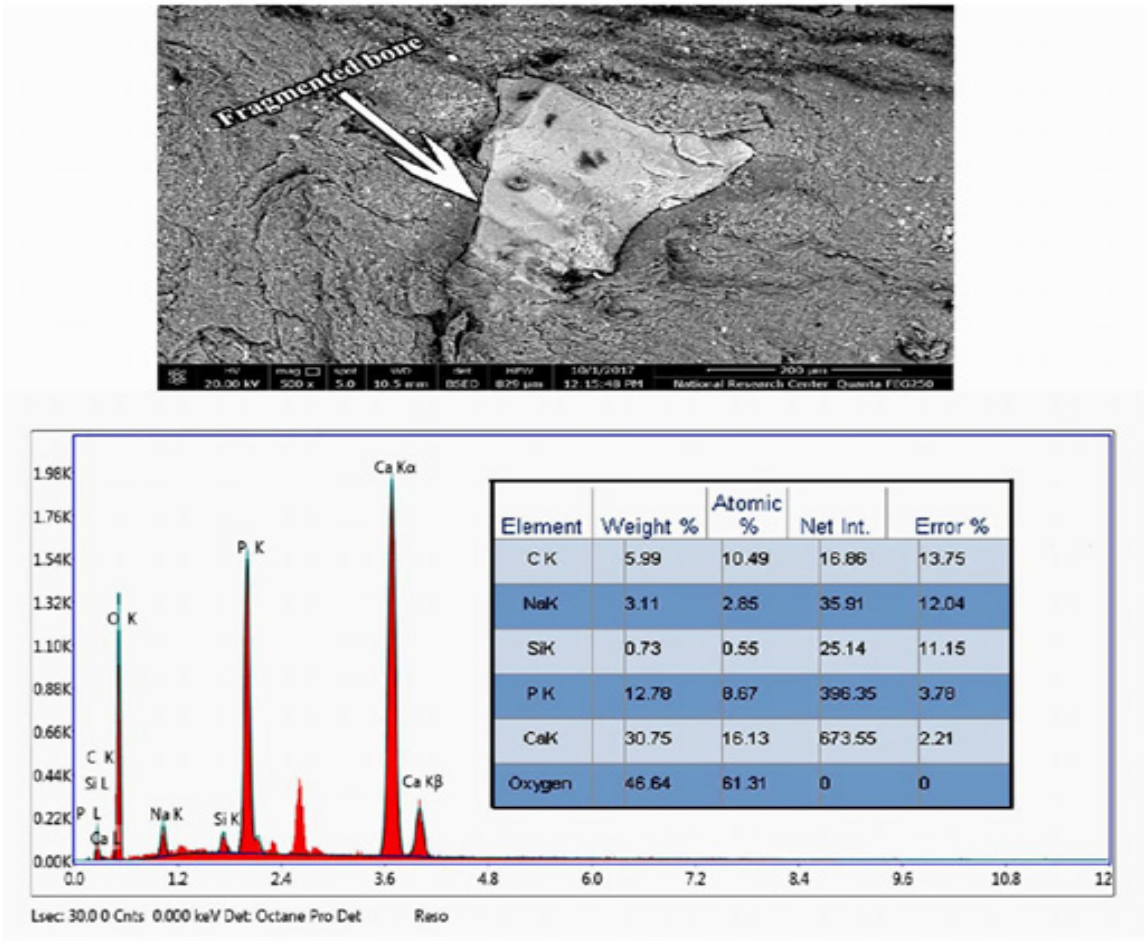

Fig. 4. SEM image and EDX analysis data showing a bone fragment in the matrix, where P content reaches 12 %, (Um El-Hwutat mine).

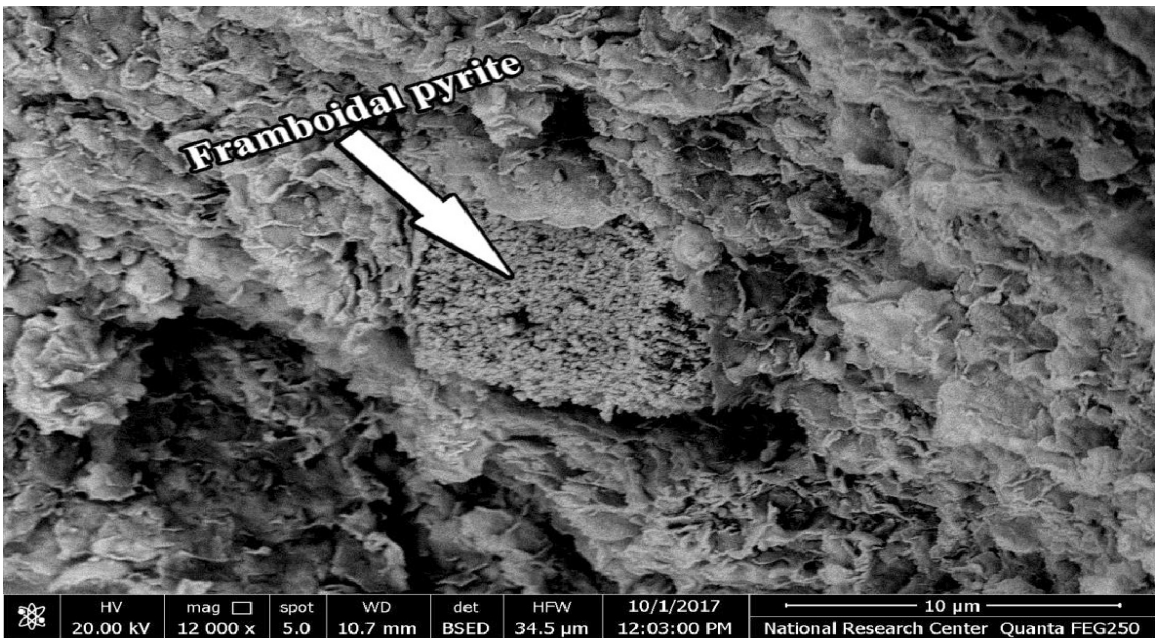

Fig. 5. SEM photograph showing spheres of framboidal pyrite (authigenic) embedded in the matrix, (Yunis mine).

Geochemistry

Geochemical composition of the major, trace and rare earth elements for the studied phosphatic rocks within the Yunis and Um El-Hwutat mines, all along with their ratios are quoted in Table 1]. The interrelationships between elements are shown in Table 2. The major and trace elemental compositions of the phosphatic rocks in these study region are compared with the published averages phosphatic rocks in Table 3.

Chemical analysis (Table 1) showed that the Ynuis phosphate mine is characterized by a high concentration of organic matter representing by loss of ignition (37.11 and 15.27% for Y-POSh and Y-OP; respectively) and low CaO (16.41 and 33.64%; respectively when compared to the Umm Al-Huwaitat mine 8.79% for loss of ignition and 42.98% for CaO. This may be due to the possibility of environmental conditions, which explains why phosphate content is low in Yunis.

Major Oxides (%) and Trace Elements (ppm)

Yunis Phosphatic rocks were defined as a high organic black shale phosphatic rocks high content in loss of ignition and a low percentage of phosphate and calcium content (OShP), and a relatively high organic, calcium and phosphate content (OCP). Therefore, phosphatic rocks for Yunis mines are classified as low-grade ore, but Um El-Hwutat mines phosphatic rocks relatively have low content in loss of ignition and a high percentage of CaO and P_2O_5 content (OP). Thus, phosphate rocks for um El-Hwutat mines are classified as good-grade ore.

The entire major, trace and rare earth elements demonstrate greatly varied distribution in the chemical composition for Yunis mines. P_2O_5 content are average 5.62 and 19.29% for Yunis organic black shale phosphatic rocks (OShP) and organic calci phosphatic rocks (OCP); respectively. P_2O_5 content is average 25.73% for Um El-Hwutat phosphatic rocks (Table 1). The Yunis value is comparable to (19.99%) [17], lower than averages of phosphatic rocks of Red Sea region (23.65 and 19.3 %) [9, 18]; respectively and (25.67 %) of Geble Duwi mine [15] (Fig. 6). Um El-Hwutat average P_2O_5 (25.73%) higher than the average values 17.86, 25.65 and 19.3% [17, 9, 18]; respectively but is relatively comparable (27.7 %) to that signed by Abou El-Anwar, et al., [14]. Phosphate rocks for Yunis are classified as low-grade ore (5.26-19.29% P_2O_5) and those of Um El-Hwutat classified to high-grade ore (23.84-289% P_2O_5) according to Ozer, et al., [19] and Gabriel [7]. More than 20% of P_2O_5 indicated that of minerals of the apatite group, such as hydroxyl-fluorapatite, carbone fluorapatite. Therefore, the composition of the studied phosphatic rocks is mainly fluorapatite and is in conformity with the obtained XRD results.

CaO recorded 16.41 and 33.64 % as average in the studied samples from Yunis mines, and 42.98% as average for those from Um El-Hwutat mines (Table 1). CaO average of Yunis phosphatic mines is lower than (28.67%) given by Abd El-Gabar and Khalifa [17], but Um El-Hwutat average is higher than (35.57%) that recorded by Abd El-Gabar and Khalifa [17]. The average CaO /P_2O_5 for Yunis mines are (2.92 and 1.81), and (1.68) for Um El-Hwutat mines; respectively (Table 1) (Fig. 6). They are higher comparable to the pure fluorapatite (1.317). The strong positive relation (r = 0.94) between Ca and P_2O_5 (Table 2 and R^2 =0.89 Fig. 6) is indicated that the presence of most Ca in apatite structure and the other part present as a cement as resulting of late diagenesis [20].

SiO_2 and Al_2O_3 average (20.805, 14.96% and 5.85, 4.62%); respectively for OShP and OP Yunis mines are higher than those recorded by Abd El-Gabar and Khalifa [17], Baioumy and Tada [9], El-Taher [18] and Abou El-Anwar, et al. [14]; respectively. But those for Um El-Hwutat phosphatic rocks (4.56 and 0.45%; respectively) are lower than the above authors. Strong positive correlation (r=0.97) between SiO_2 and Al_2O_3 indicated that occurrence of clay minerals (Table 2).

Na_2O and K_2O average (0.225, 0.27 % and 0.45, 0.48%); respectively for OShP and OP Yunis mines are lower than those recorded by Abd El-Gabar and Khalifa [17], Baioumy and Tada [9], El-Taher [18] and Abou El-Anwar, et al. [14]; respectively. But those for Um El-Hwutat phosphatic rocks (0.94 and 0.08%); respectively). Um El-Hwutat phosphatic rocks are higher in Na_2O content than those recorded for above authors. The negative correlation (r=-0.53) between Na_2O and K_2O indicated that may be different source (Table 2).

Fe_2O_3 average (1.96 and 2.15 %); respectively for OShP and OP Yunis mines are higher than those recorded by Abd El-Gabar and Khalifa [17], but MgO average (1.81 and 0.84%; respectively) were lower than given by them. In contrast, average Fe_2O_3 (1.37 %) for Um El-Hwutat is lower and MgO (1.37%) is higher than that recorded by Abd El-Gabar and Khalifa [17].

SO_3 average (8.33 and 5.87 %) for OShP

TABLE 1. XRF data major (%), trace and rare earth elements (ppm), elemental ratios and CIA of selected studied samples in the phosphatic rocks of Qusseir-Safaga region.

	Y-POSh 1	Y-POSh 2	Mean Y-POSh	Y-OSP1	Y-OSP 2	Y-SP 3	Y-SP 4	Mean Y-OP	Hwutat-CP 1	Hwutat-CP 2	Hwutat-CP 3	Hwutat-CP 4	Mean Hwutat-CP
P_2O_5	4.54	6.7	5.62	14.54	16.7	23.4	22.51	19.29	28.9	25.77	24.4	23.84	25.73
SiO_2	19.27	22.34	20.805	13.57	14.52	16.62	15.11	14.96	4.12	4.84	4.6	5.04	4.65
Al_2O_3	5.41	6.29	5.85	4.51	4.29	4.26	5.42	4.62	0.62	0.38	0.36	0.45	0.45
TiO_2	0.22	0.23	0.225	0.24	0.24	0.02	0.25	0.19	0.07	0.03	0.03	0.04	0.04
CaO	15.14	17.68	16.41	34.14	32.68	34.21	33.51	33.64	44.4	43.29	44.71	39.52	42.98
MgO	0.81	2.81	1.81	0.82	2.91	0.41	0.84	1.25	1.43	1.3	1.24	1.51	1.37
Fe_2O_3	1.95	1.97	1.96	1.98	1.98	3.09	1.54	2.15	2.02	0.78	0.71	1.95	1.37
Na_2O	0.22	0.23	0.225	0.24	0.23	0.05	0.54	0.27	0.01	1.41	1.36	0.98	0.94
K_2O	0.63	0.24	0.435	0.45	0.24	0.62	0.61	0.48	0.07	0.08	0.08	0.09	0.08
SO_3	8.71	7.95	8.33	5.81	5.75	5.97	5.95	5.87	7.41	11.66	13.16	12.97	11.30
F	0.19	1.14	0.665	1.39	1.54	1.37	1.41	1.43	1.53	1.18	0.88	1.65	1.31
Cl	0.08	0.54	0.31	0.09	0.44	0.59	0.84	0.49	0.11	0.75	0.75	0.95	0.64
L.O.I.	42.78	31.44	37.11	21.95	18.43	9.35	11.34	15.27	9.22	8.31	7.38	10.95	8.97
Tot	99.95	99.56	99.755	99.73	99.95	99.96	99.87	99.88	99.91	99.78	99.66	99.94	99.82
Mn	352	920	636	352	920	1018	1542	958	933	313	310	412	492
Mo	441	390	415.5	90	82	40	30	61	14	13	17	15	15
Sr	194	510	352	194	192	310	351	262	1375	1231	1235	1310	1288
Ba	37	41	39	38	45	33	50	42	114	52	54	152	93
Co	22	24	23	23	21	17	18	20	12	11	13	11	12
Cu	101	112	106.5	105	110	85	95	99	39	37	43	46	41
Ni	66	77	71.5	59	80	50	62	63	52	43	42	55	48
Pb	44	27	35.5	43	30	35	51	40	45	21	30	52	37
Zn	223	129	176	233	125	81	195	159	129	392	398	410	332
V	1168	1524	1346	468	424	210	220	331	200	210	185	194	197
Cr	124	141	132.5	143	152	122	136	138	92	94	85	79	88
Cd	62	53	57.5	53	61	45	47	52	11	6	7	5	7
Zr	45	55	50	45	55	37	64	50	21	23	22	27	23
As	16	14	15	14	16	13	12	14	9	10	12	11	11
Se	64	61	62.5	64	61	57	64	62	18	14	43	22	24
Rb	21	15	18	19	15	19	20	18	31	8	9	11	15
Y	8	55	31.5	8	55	123	95	70	25	20	43	48	34
Nb	4	5	4.5	4	5	3	4	4	13	14	10	11	12
U	51	44	47.5	60	42	40	56	50	90	101	95	102	97
Uc	3.14	0.18	7.74	21.3	27.1	49.57	46.41	36.4	64.98	58.84	57.64	48.1	57.4
CaO/ P_2O_5	3.33	2.64	**2.92**	2.35	1.96	1.46	1.49	1.81	1.54	1.68	1.83	1.66	1.68
V/Ni	17.70	19.79	**18.83**	7.93	5.30	4.20	3.55	**5.27**	3.85	4.88	4.40	3.53	**4.11**
V/Mo	2.65	3.91	**3.24**	5.20	5.17	5.25	7.33	**5.46**	14.29	16.15	10.88	12.93	**13.37**
V/ (V+Ni)	0.95	0.95	**0.95**	0.89	0.84	0.81	0.78	**0.84**	0.79	0.83	0.81	0.78	**0.80**
V/ (V+Cr)	0.90	0.92	**0.91**	0.77	0.74	0.63	0.62	**0.71**	0.68	0.69	0.69	0.71	**0.69**
CIA	85.51	92.52	**89.015**	83.06	85.97	82.40	81.45	**83.22**	87.32	11.85	11.39	18.00	**32.14**

Y-POSh: phosphorite dominated Organic shale
Y-OSP: Organic shale phosphorite
Hwutat-CP: Calcareous phosphorite

TABLE 2. Correlation coefficient between elements for the studied samples.

	P2O5	SiO2	Al2O3	TiO2	CaO	MgO	Fe2O3	Na2O	K2O	SO3	F	Cl	L.O.I.	Tot	Mn	Mo	Sr	Ba	Co	Cu	Ni	Pb	Zn	V	Cr	Cd	Zr	As	Se	Rb	Y	Nb	U
P2O5	1.00																															
SiO2	-0.82	1.00																														
Al2O3	-0.77	0.97	1.00																													
TiO2	-0.71	0.71	0.82	1.00																												
CaO	0.94	-0.91	-0.85	-0.68	1.00																											
MgO	-0.27	0.15	0.11	0.31	-0.20	1.00																										
Fe2O3	-0.21	0.51	0.47	0.13	-0.37	-0.10	1.00																									
Na2O	0.40	-0.62	-0.65	-0.50	0.51	-0.06	-0.83	1.00																								
K2O	-0.45	0.73	0.77	0.48	-0.58	-0.50	0.52	-0.53	1.00																							
SO3	0.27	-0.62	-0.72	-0.63	0.36	-0.01	-0.63	0.85	-0.63	1.00																						
F	0.59	-0.33	-0.24	-0.15	0.55	0.23	0.23	-0.08	-0.32	-0.22	1.00																					
Cl	0.43	-0.28	-0.31	-0.40	0.35	0.06	-0.33	0.68	-0.26	0.51	0.31	1.00																				
L.O.I.	-0.96	0.74	0.68	0.67	-0.93	0.19	0.22	-0.44	0.43	-0.24	-0.66	-0.56	1.00																			
Tot	0.24	-0.10	-0.07	-0.12	0.09	-0.30	0.47	-0.30	0.31	-0.23	0.14	-0.09	-0.10	1.00																		
Mn	0.13	0.38	0.47	0.33	-0.12	0.11	0.38	-0.49	0.38	-0.65	0.40	0.15	-0.16	0.20	1.00																	
Mo	-0.93	0.75	0.66	0.54	-0.94	0.24	0.19	-0.38	0.36	-0.14	-0.70	-0.43	0.96	-0.23	-0.10	1.00																
Sr	0.67	-0.87	-0.92	-0.76	0.70	0.02	-0.50	0.61	-0.83	0.76	0.21	0.37	-0.59	-0.12	-0.33	-0.48	1.00															
Ba	0.49	-0.65	-0.65	-0.44	0.46	0.08	-0.02	0.20	-0.58	0.47	0.46	0.26	-0.38	0.29	-0.12	-0.38	0.72	1.00														
Co	-0.87	0.90	0.92	0.86	-0.83	0.24	0.38	-0.62	0.60	-0.66	-0.29	-0.49	0.78	-0.22	0.20	0.70	-0.89	-0.66	1.00													
Cu	-0.78	0.92	0.96	0.86	-0.80	0.23	0.47	-0.64	0.68	-0.73	-0.16	-0.35	0.68	-0.06	0.36	0.60	-0.95	-0.63	0.96	1.00												
Ni	-0.71	0.73	0.75	0.83	-0.73	0.65	0.36	-0.58	0.27	-0.55	0.00	-0.28	0.66	0.01	0.37	0.60	-0.65	-0.24	0.78	0.83	1.00											
Pb	0.07	-0.04	0.07	0.18	-0.02	-0.42	0.32	-0.29	0.34	-0.16	0.16	-0.10	0.04	0.49	0.23	-0.09	-0.06	0.50	-0.04	0.03	0.04	1.00										
Zn	0.29	-0.65	-0.67	-0.45	0.44	-0.17	-0.73	0.92	-0.49	0.89	-0.13	0.49	-0.28	-0.20	-0.68	-0.29	0.61	0.38	-0.58	-0.63	-0.57	-0.03	1.00									
V	-0.92	0.75	0.66	0.57	-0.91	0.40	0.17	-0.37	0.24	-0.16	-0.55	-0.37	0.90	-0.40	-0.05	0.97	-0.44	-0.37	0.73	0.62	0.66	-0.19	-0.32	1.00								
Cr	-0.63	0.83	0.90	0.86	-0.64	0.27	0.39	-0.63	0.61	-0.83	-0.01	-0.37	0.52	-0.06	0.45	0.43	-0.92	-0.68	0.91	0.95	0.78	-0.08	-0.69	0.48	1.00							
Cd	-0.77	0.92	0.95	0.83	-0.80	0.14	0.50	-0.70	0.75	-0.77	-0.25	-0.46	0.70	0.08	0.35	0.61	-0.97	-0.67	0.94	0.98	0.78	0.04	-0.69	0.59	0.94	1.00						
Zr	-0.60	0.82	0.91	0.89	-0.68	0.25	0.29	-0.48	0.64	-0.68	-0.02	-0.08	0.49	-0.03	0.59	0.44	-0.84	-0.52	0.81	0.91	0.81	0.14	-0.55	0.47	0.90	0.86	1.00					
As	-0.83	0.78	0.76	0.68	-0.76	0.24	0.32	-0.42	0.55	-0.42	-0.42	-0.35	0.74	0.03	-0.02	0.64	-0.85	-0.61	0.85	0.86	0.72	-0.10	-0.38	0.59	0.76	0.87	0.67	1.00				
Se	-0.69	0.86	0.90	0.76	-0.70	0.01	0.37	-0.52	0.77	-0.64	-0.29	-0.28	0.57	-0.09	0.34	0.51	-0.93	-0.71	0.89	0.92	0.63	0.08	-0.53	0.49	0.85	0.91	0.84	0.85	1.00			
Rb	-0.02	0.19	0.27	0.27	-0.15	-0.22	0.53	-0.80	0.35	-0.64	0.06	-0.68	0.18	0.37	0.46	0.13	-0.21	0.07	0.21	0.19	0.18	0.51	-0.69	0.07	0.22	0.29	0.15	-0.05	0.15	1.00		
Y	0.25	0.28	0.27	-0.13	0.02	-0.11	0.45	-0.18	0.38	-0.32	0.36	0.52	-0.38	0.22	0.72	-0.26	-0.25	-0.15	-0.01	0.19	0.04	0.05	-0.41	-0.23	0.19	0.16	0.33	0.00	0.29	0.00	1.00	
Nb	0.64	-0.88	-0.91	-0.67	0.70	0.09	-0.56	0.61	-0.85	0.70	0.20	0.25	-0.53	-0.06	-0.39	-0.46	0.95	0.64	-0.85	-0.92	-0.59	-0.16	0.60	-0.43	-0.83	-0.91	-0.82	-0.81	-0.96	-0.21	-0.41	1.00
U	0.64	-0.93	-0.93	-0.67	0.73	-0.14	-0.63	0.74	-0.74	0.81	0.14	0.35	-0.55	-0.08	-0.51	-0.52	0.93	0.68	-0.87	-0.93	-0.72	0.04	0.81	-0.52	-0.90	-0.95	-0.82	-0.79	-0.88	-0.31	-0.41	0.92

TABLE 3. The trace elemental composition of the phosphates in the current study as compared with published average phosphates in different countries.

Element	Y-POSh	Y-OP	Hwutat-CP	G.Duwi Mine	Tunisia	Morocco	Jordan	AWP	ASC	Soil EC	Fertilizer C.
As	15	14	11	19.6	11	10.7	n.d	23	13	8	75
Cd	57.5	52	7	n.d	50.3	21.6	23	1711	0.3	1.5	20
Co	23	20	12	2.6	0.3	0.75	0	7	19	n.d	150
Cr	132.5	138	88	161.4	42.7	217	51	125	90	60	n.d
Mn	636	958	492	422	51.2	15	n.d	n.d	850	n.d	n.d
Mo	415.5	61	15	323.4	14.1	7.9	0	23	2.5	n.d	20
Ni	71.5	63	48	72	55	41.4	15	53	68	50	180
Pb	35.5	40	37	n.d	3	6.3	4	10	20	100	500
Sr	35.2	262	1288	1705	1606	1331	n.d	1900	300	n.d	n.d
U	47.5	50	97	35	40	150.7	27	380	3	3	n.d
V	1347	331	197	246	n.d	n.d	n.d	25	n.d	n.d	n.d
Zn	176	159	332	149	226	279	121	195	95	200	1850
Zr	50	50	23	n.d	n.d	n.d	n.d	n.d	n.d	n.d	n.d

G. Duwi mine (14), Tunisia, Morocco (50); Jordan (51); AWP (31); ASC: Average Shale Composition by Turekian and Wedepohl (30); Soil EC: Permissible limit established by the Soil EC Directive (52), Fertilizer Canada: Permissible limit established by the Canadian Food Inspection Agency (49).

Note: n.d. = not determined.

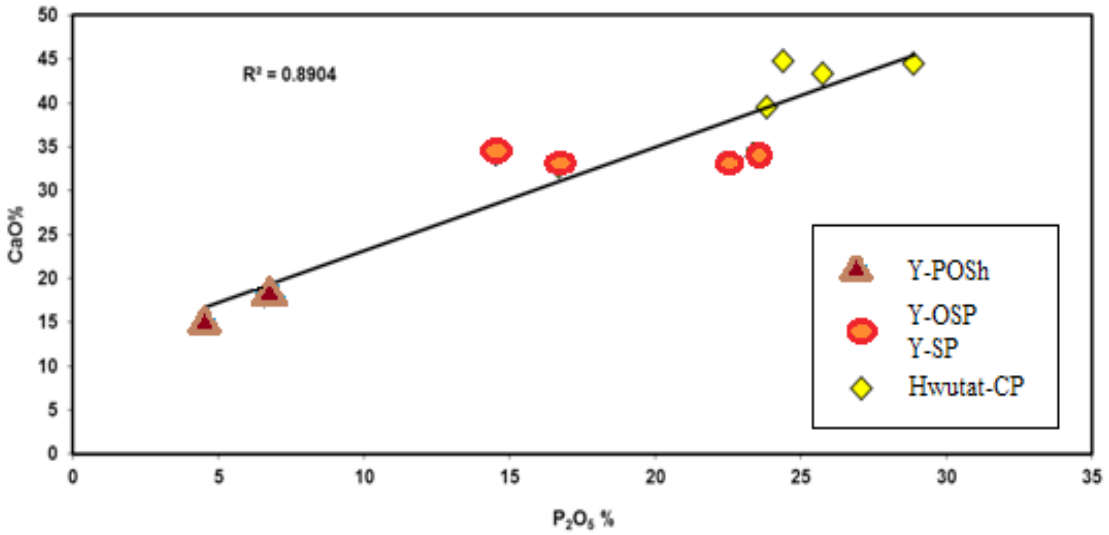

Fig. 6. The relation between P2O5 and CaO for the major oxides in the studied phosphatic rock.

and OP Yunis mines, and (11.3%) is average for Um El-Hwutat mines. The SO_3 average of Yunis phosphatic samples are lower than for Um El-Hwutat in the study region. The negative correlation (r=-0.63) between Fe_2O_3 and SO_3 content indicates that the absence of pyrite [21, 14]. The relatively high negative correlation (r=-0.63) between Fe_2O_3 and SO_3 and high positive correlation (r=O.85) between Na_2O and SO_3 may be indicated no pyrite content but salt are source.

The high average losses of ignition (37.11 and 15.27%); respectively for OShP and OP Yunis mines, and (8.97%) for average of Um El-Hwutat samples are also in Table 1. The strong negative correlation (r=-0.96 and r=-093) between L.O.I and P_2O_5, CaO are revealed that the presence of large quantity of organic matter and subjected to intensive chemical weathering [22].

The enrichment of the trace and rare earth elements in sediments may be resulting from diagenesis, hydrothermal or sea water. The trace and rare earth elements content; Mn, Mo, Co, Cu, Cr, Cd, Ni, V, Zr, As, Se, Rb and Y in Yunis mines average (636 and 958 ppm, 415.5 and 61 ppm, 23 and 20 ppm, 106.5 and 99 ppm, 132.5 and 138ppm, 57.5 and 52ppm, 71.5 and 63ppm, 1346 and 331ppm, 50 and 50 ppm, 15 and 14ppm, 62.5 and 62ppm, 18 and 18ppm, 31.5 and 70ppm are more enriched than those in Um El-Hwutat mine (Table 1).

But, the Um El-Hwutat average phosphatic rocks are enriched in Sr, Ba, Pd, Nb, Zn and U (1288, 93, 37, 12, 332 and 97ppm; respectively) than those for Yunis average phosphatic rocks. The studied two mines are comparable in Ni content (Table 3 and Fig. 7). Generally, the two studied mines are more enriched than those in the UCC [23].

REE compositions of the phosphatic rocks have been modeled previously to assess the mechanism of REE uptake and subsequent alteration during diagenesis [24, 25] and identify sequential the palaeo-seawater REE compositions [26, 27]. Thus, REE incorporation was phosphatic rocks attributed to either adsorption or substitution mechanisms during diagenesis [28, 29].

P_2O_5 has positive correlation with Sr, Nb. U, Ba, Zn, Y and Pb (r= 0.67, 0.64, 64, 49, 0.29, 0.25 and 0.07; respectively, Table 2), which indicates that these trace and rare earth elements are associated with phosphatic rocks. SiO_2 has positive correlation with Cd, Cu, Co, Se, Cr, Zr, As, V, Mo, Ni, Mn, Y, Rb and TiO_2, (r=92, 0.92, 0.90, 0.86, 0.83, 0.82, 0.78, 0.75, 0.75, 0.73, 0.38, 0.19 and 0.71; respectively) which revealed that these elements may be associated with the detrital quartz.

V, Cr, Cd, Zr, As, Se, Y and Nb are positively correlated with SiO_2, Al_2O_3, Fe_2O_3 TiO_2 and with each other, which revealed that these elements may be associated with the detrital quartz, clay minerals, iron oxides or with the heavy minerals rather than with apatite (Table 2).

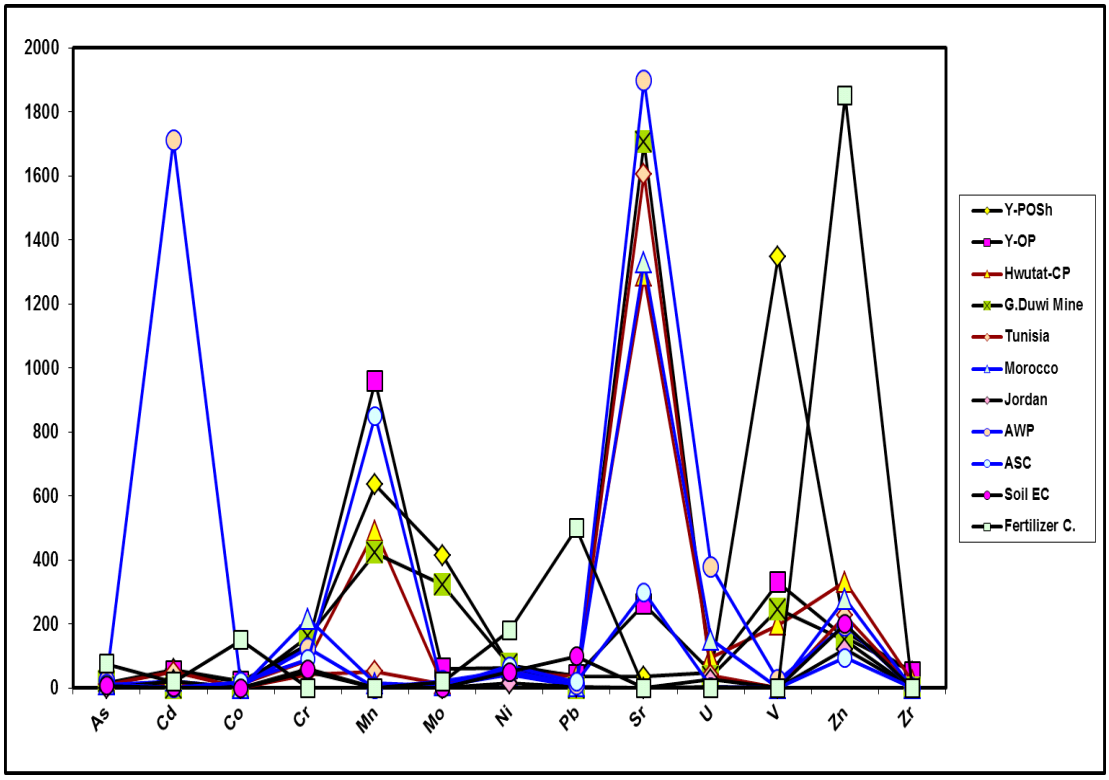

Fig. 7. Concentrations of some trace elements in the average studied phosphatic rocks with other areas.

Distribution of Uranium

U average content in the studied samples are 47.5, 50 and 97ppm from Yunis OShP, OP and Um El-Hwutat mines; respectively (Table 1). These values are higher than U content in the earth's crust (2.7ppm) and the shale sediments (3.0 ppm), [30]. U average content from Yunis mines is lower than is recorded in Um El-Hwutat phosphatic studied samples. This could be attributed to the post-depositional enrichment of uranium in Qussier than Safaga.

Table 2 shows that U has strong positive correlation with Sr, high and high relatively positive correlation with CaO and P_2O_5 (r= 0.93, 0.73 and 0.64; respectively), which indicate that uranium was best associated with these elements in phosphate minerals.

The high (r= 0.64 and 0.73; respectively) positive correlation of U with P_2O_5 and CaO indicated that the important role of phosphate in fixation of U^{6+} as uranyle ion $(UO_2)^{2+}$. Thus, the secondary uranium minerals such as phosphuranylite $\{Ca\ (UO_2)\ (PO_4)_2(OH)_2\ 6H_2O\}$ may be precipitated. The high positive correlation (r= 0.73) between CaO and U indicated that part of the U content occurs as tetravalent state U^{4+} substituting for Ca^{2+} in the phosphate minerals during subaerial weathering [31]. Also, the high and moderate positive (r=0.67 and 0.40; respectively) correlation between P_2O_5 with Sr and Na_2O are may be possibly related to the occurrence of belovite $\{Sr_3(CeNaCa)_2(PO_4)_3OH\}$ mineral. Thus, phosphuranylite and belovite may be deposited in the study regions as secondary minerals.

U is strong positive correlated with Nb and Zn (r= 0.92 and 0.81; respectively) and high positive correlated with Ba (r= 0.68). Therefore, U may be released during the weathering and behave as immobile and it can be fixed rapidly in new phases [32].

U in the studied samples is strong and negative correlation with some heavy element such as Cd, Cu, Cr, Co, Zr, As, Ni and V (r=-0.95,-0. 93,-0.90, -087, -0.82, -0.72, -0.72 and -0.58; respectively). Thus, U contents in the study phosphatic rocks were probably associated with anoxic sediments more than associated with the heavy metals and trace elements during the chemical weathering [33- 35] under oxic conditions [36]. Thus, anoxic sediments are much more enriched in U than oxic ones [37].

Akyuz, et al, [38] studied geochemistry of Mardin-Mazidag Phosphate Deposit using the quadratic regression models of Narula and Wellington [39], which widely used in many practices, where allow description of the objects in comparatively wide area of the input variable changes and that expressed generally as follows:

$$\hat{y} = b_0 + \sum_{i=1}^{m} b_i x_i + \sum_{i=1}^{m} b_i x_i^2$$

Based on real data consisting of Mardin-Mazidag Phosphate Deposit observations, since Y represent the U concentration in mg/kg and the two predictor variables X1, X2 that represent P_2O_5 and F concentration in %; respectively, [38] distinguished the relation between Phosphate, Fluorite and Uranium. After the regression analysis for them experiment, the following mathematical model was obtained:

$$\mathbf{Y = -\,8.9614 + 3.0972\ X_1 - 10.1493\ X_2}$$

As a result the interrelation between P_2O_5 F and U concentrations of the phosphate ore samples could be expressed as follows:

$$\mathbf{U_{(mg/kg)} = -\,8.9614 + 3.0972\ \ P_2O_{5(wt.\%)} - 10.1493\ F_{(wt.\%)}}$$

Where U, P_2O_5 and F concentrations represent the Y, X_1 and X_2 respectively in the quadratic regression model.

The calculated U(mg/kg) for Yunis and Um El-Hwutat according [38] found in Table 1.

The 3-D pyramids plotting of measured uranium (U_m) in ppm, calculating uranium U.c [41] in ppm, P_2O_5 and F as wt.% showing in Fig. 8. The U_m and U_c within Yunis samples with high P_2O_5 are strongly matched to each other. Thus, the studied Yunis phoshatic samples have low P_2O_5 and high organic matter. The U_m have high value versus to the U_c, which support that anoxic sediments are much more enriched in U than oxic ones in Yunis phosphates mines.

The values of the studied samples are higher than Uc values; this could be attributed to the post-depositional enrichment of uranium. Consequently, Uranyl carbonates and Uranyl sulfates may be deposited in Um El-Hwutat regions as secondary minerals.

Depositional Environmental

V, Ni, Mo, U, Cu, Cr, Re, Cd, Sb and Tl are considered as redox-sensitive trace elements in marine sediments and indicate for paleo-oceanographic conditions [40- 42]. The redox-sensitive metals are highly enriched in anoxic sediments.

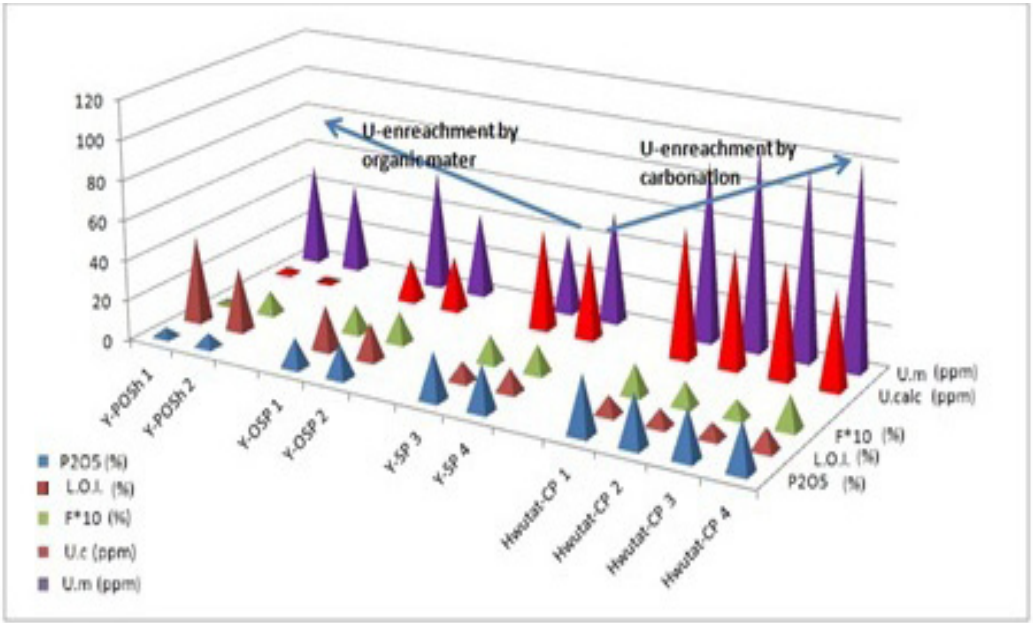

Fig. 8. 3-D pyramids plotting showing the Yunis and Um El-Hwutat concentration data series of U.m (measured uranium) in ppm, U.c (calculating uranium after (38) Ucalc.(mg/kg) = – 8.9614 + 3.0972 P_2O_5(%) – 10.1493 F(%)) in ppm, P_2O_5 in wt.% and F in wt.%.

The average redox-sensitive trace elements (V, Mo, U, Cu, Cr, Se, Cd, Co and Zn) in the studied phosphatic rocks from Yunis mines (1364, 415.5, 47.5, 106.2, 132.5, 62.5, 57.5, 23 and 176ppm; for OShP, also 331, 61, 50, 99, 138, 62, 52, 20 and 159ppm for OCP, as well as 197, 15, 97, 41, 88, 24, 7, 12, and 332ppm for Um El-Hwutat mines show enrichments of the redox-sensitive elements (97, 1.5, 2.5, 28, 92, 0.34, 0.098, 17.3 and 67 ppm; respectively) compared to the composition of the bulk continental crust [44]. The enrichment relative to continental crust are range from a few times as in the case of Cu, Co, Cr and Zn; to ten times for elements such as V and U; to hundreds of times in the case of Mo, and thousands of times for Cd and Se. Thus, the enrichment in the contents of the redox-sensitive elements of the Qussier-Safaga phosphatic rocks can be indicated as strong confirmation for anoxic conditions during the deposition [41, 40]. This is in agreements with [16 and 14]. The more enrichment of the most trace and rare earth elements were may be possibly due to they were leached from the above Dakhla shales in the study region. V is enriched in comparison to Ni in anoxic marine environments which may be due to the strong activity of sulfate reducing bacteria in this environment and relatively higher stability of V compared to Ni [43].

V/Mo ratio in sediments < 2, it indicates an anoxic condition, ratio between 2 to 10 indicates suboxic conditions, and it from 10 to 60 indicates normal oxygenation [44]. V/Mo ratio in the studied phosphatic samples in Yunis mines ranges from 2.65 to 5.46 lies within the range of suboxic conditions of deposition, but in Um El-Hwutat mines ranges from 10.88 to 14.29 lies within the range of oxygenation condition of deposition, (Table 1).

V/Ni ratio higher than 3 indicates that marine origin organic matter was deposited under reducing conditions, while V/Ni ratios ranging between 1.9 to 3 indicate deposition in a dysoxic-oxic environment with mixed terrigenous and marine organic matter, while V/Ni ratios less than 1.9 indicate predominantly terrigenous organic matter [45]. The Yunis phosphatic samples recorded V/Ni ratio (18.83, 5.27 for OShP and OCP; respectively) indicated that the deposition took place under reducing conditions, at the same occasion the Um El-Hwutat samples with V/Ni ratio of 4.11 indicating the possible deposited under reducing conditions also. Generally, the V/Ni ratio in the phosphatic samples for the study region range from 3.85 to 19.79 with averaging 11.82, which are greater than 3. Thus, it was indicated that these phosphatic rocks were deposited in a reducing environment (Table 1).

V/(V+Ni) and V/(V+Cr) ratios can be used to indicate oxygenation of the depositional environment, and higher V/(V+Ni) and V/(V+Cr) ratios indicate more strongly reducing conditions [46]. Pi, et al., [42] recognized V/(V+Ni) and V/(V+Cr) ratios of more than 0.89 and 0.76; respectively, to indicate strongly reducing conditions. Thus, the analyzed samples from Yunis phosphatic rocks are display more reducing nature of their depositional environment than those from Um El-Hwutat samples (Table 1).

The Chemical Index of Alteration (CIA) values in the studied samples are recorded 89.015, 83.22 and 32.14 %; respectively for Yunis and Um El-Hwutat average samples (Table 1). These average values indicated that the study rocks for Yunis mines were exposed to high intensive chemical weathering than those of the Um El-Hwutat rocks, [47, 48].

Thus, The Yunis phosphatic mines was differ from those of Um Hweitat mines not only in the quality of the ore and the concentration of the phosphate**,** but also in the nature and environment of the deposition of the ore, which confirmed by the chemical analysis of ore.

Comparison of the chemical composition with published averages of other contraries

Table 3 shows the distribution of the trace and rare earth elements in the study phosphatic rocks and in other different localities. The phosphatic rocks in Qussier-Safaga region are enrichment in V, Cr, Mo, Mn, Ni and As than all the other contraries (Table 3 and Fig. 7). The study region recorded high concentration in Zn, As and Mn than those in the Geble Duwi Mines [14]. Yunis phosphatic samples were high contents in Co and U, and Um El-Hwutat phosphatic rocks enriched in Mo than those of Geble Duwi Mines.

Table 3 and Fig. 7 show that all the elements contents are higher than those in Average World Phosphorite (AWP 31) and the Fertilization Food [49] expected Sr content. Furthermore, all the average values for the elements are higher than those in Average Shale Composition (ASC) and UCC [30, 23]. The trace elements Ni, Zn and Co values are less than those of the Fertilization

Food [49-52]. Thus, it may be concluded in the Duwi Formation, at Qussier –Safaga region the phosphatic rocks are suitable for industrialized fertilizers.

Conclusions

Mineralogical and geochemical studies for the phosphate rocks in Yunis (Qusseir) and Um El-Hwutat (Safaga) mines of the Duwi Formation at Qusseir- Safaga regions were carried out to identify the depositional environment. Mineralogicaly, the bulk samples are mainly apatite (francolites) and the non-phosphatic minerals include quartz, calcite, dolomite and clay minerals (montmorillonite).

The studied phosphatic rocks of Duwi Formation in the Qusseir-Safaga region contain high concentrations of some trace and rare earth elements such as V, Zn, Cu, Cr, Mo, Ni, Cd, U, As, Se, Y and Mn, which added significant value to the studied phosphatic rocks. They are deposited under relatively suboxic to anoxic reducing marine conditions. In comparison with the Average World Phosphorite (AWP), the Fertilization Food the studied phosphatic rocks are higher in all elements expected Sr. The values of the Chemical Indexes of Alteration (CIA) and the chemical analysis indicated that the studied phosphatic rocks for Yunis mines were subjected to high intensive chemical weathering than those of the Um El-Hwutat rocks.

Uranium occurs mainly in oxidized U^{6+} state. It possibly fixed with the phosphate ion, forming secondary uranium phosphate minerals such as phosphuranylite and belovite in the study regions. The huge amount of phosphorites in Qusseir-Safaga region, utilization of their incorporated trace elements and uranium contents must be taken into consideration.

Acknowledgements

The authors thank the National Research Centre for financial support for this work.

References

1. Peter L. Mc., Glen B. M., and Paul W. W., Uranium in early Proterozoic phosphate-rich metasedimentary rocks of east-central Minnesota. *Economic Geology* **81** (1), 173-183 (1986).
2. El-Kammar A.M., Zayed M. and Amer S.A., Rare earths of the Nile Valley phosphorites, Upper Egypt. *Chem. Geol.*, **24**, 69-81 (1979).
3. Glenn C.R. and Arthur M.A., Anatomy and origin of a Cretaceous phosphorite-greensand giant. *Egypt. Sedimentology*, **37**, 123-154 (1990).
4. El-Tarabili, E., Paleogeography, paleoecology and genesis of the phosphatic sediments in the Quseir-Safaga region. UAR. *Econ. Geol*. **64**, 172-182 (1969).
5. Youssef M.I., Upper Cretaceous rocks in Qosseir region. *Bull. Inst. Désert Égypt*. **7**(2), 35-54 (1957).
6. Sengul H. A., Ozer K. and Gulaboglu M.S., Benefication of Mardin-Mazidagi (Turkey) calcareous phosphate rock using dilute acetic acid solutions. *Chem. Eng. J.* **122**, 135–140 (2006).
7. Gabriel M. F., Phosphate rock formation and marine phosphorus geochemistry: The deep time perspective. *Chemosphere,* **84,** 759–766 (2011).
8. Said R.. The Geology of Egypt., Elsevier Pub. Co. [distributors for the U.S.: American Elsevier Pub. Co., New York]; 1st edition p. 377 (1962).
9. Baioumy H.M., Tada R., Origin of Upper Cretaceous phosphorites in Egypt. *Cretaceous Research*. **26**, 261-275 (2005).
10. Abou El-Anwar E.A. and El-Sayed M.S., Composition of black shale from Quseir, Red Sea, Egypt with emphasis on the sequential extraction of some metals, *Bull. NRC, Egypt*. **32** (2), 109-131 (2008).
11. Abou El-Anwar E.A., Petrographical, geochemical and diagenetic studies of the Middle Eocene carbonates, Mokattam Formation of Darb El-Fayium region, *(Int. Conf. on Geological Sciences and Engineering, France, Paris*. **80**, 1315-1325 (2011).
12. Abou El-Anwar, E., A., Contribution to the composition and origin of the reef Terraces in Ras Mohamed, Sharm El-Sheikh Coast, Southern Sinai, Egypt. *Geology of Egypt*. **56**, 33-48 (2012).
13. Abou El-Anwar E.A., Composition and Origin of the Dolostones of Um Bogma Formation, Lower Carboniferous, West Central Sinai, Egypt. *Carbonates and Evaporates*, (014-0188-3). (2014).
14. Abou El-Anwar E.A., Abd El Rahim, S.H.,and Mekky, H.S., Spherulitic dahllite of Duwi Formation phosphorite, *Carbonates Evaporites.* DOI 10.1007/s13146-017-0377-y.(2017).

15. Schieber J., Baird G., On the origin and significance of pyrite spheres in Devonian black shale of North America. *J. of Sedimentary Research*. **71** (1), 155-166 (2001).

16. Abou El-Anwar E.A., Mineralogical, petrographical, geochemical, diageneses and provenance of the Cretaceous Black Shales, Duwi Formation at Quseir-Safaga, Red Sea, Egypt. *Egyptian Journal of Petroleum*. **25**, 323-332. (2016).

17. Abd El-Gabar A.E, Khalifa I.H., Application of multivariate statistical analyses inthe interpretation of geochemical behaviour ofuranium in phosphatic rocks in the Red Sea, Nile Valley and Western Desert, Egypt. *Journal of Environmental Radioactivity* **61**, 169–190 (2002).

18. El-Taher A., Elemental analysis of two Egyptian phosphate rock mines by instrumental neutron activation analysis and atomic absorption spectrometry, *Applied Radiation and Isotopes,* **68**, 511-515 (2010).

19. Ozer, A. K., Gulaboglu, M. Bayrakceken, S., 2000, Physical structure and chemical and mineralogical composition of the Mazidagi (Turkey) phosphate rock, *Ind. Eng. Chem. Res.* **39**, 679–683 (2011).

20. Einsale, G., Sedimentary basins: Evolution, facies, and sediment budget (p. 628). Berlin, Heidelberg: Springer (1992).

21. Xiugen, Fu., Wang, Y., Zeng, F., Tan, E., and Feng, X., RE of marine oil shale from the Changshe Mountain Tibet, China. *Int J Coal Geol.* **81**, 191–199 (2010).

22. Blumenberga M., Thiela V., Riegela W., Linda, K. and Joachim R., Biomarkers of black shales formed by microbial mats, Late Mesoproterozoic (1.1 Ga) Taoudeni Basin, Mauritania. *Precambrian Research*. **196-197**, 113-127 (2012).

23. Rudnick,, RL., Gao S., Composition of the Continental Crust. *Treatise On Geochemistry*. **3**, 1-64 (2003)

24. Chen J., Algeo T.J., Zhao L., Chen Z.-Q., Cao L., Zhang, L., and Li, Y., Diagenetic uptake of rare earth elements by bioapatite, with an example from Lower Triassic conodonts of South China. *Earth Sci. Rev*. **149**, 181–202 (2015).

25. Zhang L., Algeo T.J., Cao L., Zhao L., Chen Z.-Q., and Li, Z., Diagenetic uptake of rare earth elements by condone apatite. *Palaeogeogr. Palaeoclimatol. Palaeoecol*. **458,** 176–197 (2016).

26. Lécuyer C., Reynard B., and Grandjean, P., Rare earth element evolution of Phanerozoic seawater recorded in biogenic apatites. *Chem. Geol*. **204**, 63–102 (2004).

27. Abbott A.N., Haley B.A., McManus J., and Reimers, C.E., The sedimentary flux of dissolved rare earth elements to the ocean. *Geochim. Cosmochim. Acta.* **154**, 186–200 (2015).

28. McArthur J.M., and Walsh J.N., Rare-earth element geochemistry of phosphorites. *Chem. Geol*. **47**, 191–220 (1985).

29. Kohn M.J., and Moses R.J., Trace element diffusivities in bone rule out simple diffusive uptake during fossilization but explain in vivo uptake and release. *Proc. Natl. Acad. Sci*. **110,** 419–424 (2013).

30. Turekian K.K., and Wedepohl, K.H., Distribution of the elements in some major units of the earth,s crust. *Bull. Geol. Soc. Am*. **72**, 175-192 (1961).

31. Altschuler Z.S., The geochemistry of trace elements in marine phosphorites. Part I. Characteristis abundances and enrichment. *The Society of Economic Paleontologists and Mineralogists (SEPM) vol 29 S*EPM Spec Publ, Tulsa, pp 19–30 (1980).

32. Venter R., and Boylett M., The evaluation of various oxidants used in acid leaching of uranium. *Hydrometallurgy Conference. The Southern African Institute of Mining and Metallurgy*. 445-456. (2009).

33. Waite T.D., Davis J.A., Payne T.E., Waychunas G.A., Uranium (VI) adsorption to ferrihydrite: application of a surface complexation model. *Geochim Cosmochim Acta* **58**, 5465–5478 (1994).

34. Bots P., and Behrends T., Uranium mobility in subsurface aqueous systems: the influence of redox conditions. *Mineralogical Magazine,* **72**, 381-384 (2008).

35. Bata, T., Evidences of Widespread Cretaceous Deep Weathering and Its Consequences: A Review, *Earth Science Research.* **5**, (2), (2016)

36. Song H.J.,Wignall P.B., Tong J.N., Bond D.P.G., Song H.Y., Lai X.L., Zhang K., Wang H.M., and Chen Y.L., Geochemical evidence from bio-apatite for multiple oceanic anoxic events during Permian–Triassic transition and the link with end-Permian extinction and recovery. *Earth Planet. Sci. Lett.* 323–324, 12–21. (2012).

37. Wignall P.B., and Twitchett R.J., Oceanic anoxia and the end Permian mass extinction. *Science*. **272**, 1155-1158 (1996).

38. Akyuz T., Akyuz S., Calglar H., and Calgar N., FT-IR, EDXRF Analysis of the Mardin-Mazidag Phosphate Deposit of Turkey and Relations between Phosphate, Uranium and Fluorine. *Asian Journal of Chemistry* **20** (5), 4085-4091(2008).

39. Narula S., and Wellington J., Multiple Criteria Linear Regression. *European Journal of Operational. Research* **181** (2), 767-772 (2007).

40. Pattan, J.N., and Pearce, N.J.G., Bottom water oxygenation history in southeastern Arabian Sea during the past 140 ka: results from redox-sensitive elements. *Palaeogeography, Palaeoclimatology, Palaeoecology*. **280**, 396-405 (2009).

41. Adegoke A.K., Abdullah W.H., Hakimi M.H., Yandoka B.M.S., Mustapha K.A., and Aturamu, A.O., Trace elements geochemistry of kerogen in Upper Cretaceous sediments, Chad (Bornu) Basin, northeastern Nigeria: Origin and paleo-redox conditions. *Journal of African Earth Sciences.* **100**, 675-683 (2014).

42. Pi D.H., Jiang S.Y., Luo L., Yang J.H., and HF Hong-Fei Ling Depositional environments for stratiformwitherite deposits in the Lower Cambrian black shale sequence of the Yangtze Platform, southern Qinling region, SW China: Evidence from redox-sensitive trace element geochemistry. *Palaeogeography, Palaeoclimatology, Palaeoecology,* **398**, 125-131 (2014).

43. Peters K.E., and Moldowan, J.M., The Biomarker Guide: Interpreting Molecular Fossils in Petroleum and Ancient Sediments. Prentice-Hall, Inc., Englewood Cliffs, New Jersey. (1993).

44. Gallego-Torres D., Martinez-Ruiz F., De Lange G. J., Jimenez-Espejo F. J., and Ortega-Huertas, M., Trace-elemental derived paleoceanographic and paleoclimatic conditions for Pleistocene Eastern Mediterranean sapropels. *Palaeogeography, Palaeoclimatology, Palaeoecology.* **293**(1), 76-89 (2010).

45. Galarraga F., Reategui K., Martïnez A., Martínez M., Llama, J.F., and Márquez, G., V/Ni ratio as a parameter in palaeoenvironmental characterisation of non-mature medium-crude oils from several Latin American basins. *Journal of Petrological Science and Engeneering,* **61**, 9-14 (2008).

46. Zhou C.M., and Jiang S.Y., Palaeoceanographic redox environments for the lower Cambrian Hetang Formation in South China: Evidence from pyrite framboids, redoxsensitive trace elements, and sponge biota occurrence. *Palaeogeography, Palaeoclimatology, Palaeoecology.* **271**, 279-286 (2009).

47. Fedo C.M., Eriksson K., and Krogstad E.J., Geochemistry of shale from the Archean (~ 3.0 Ga) Buhwa Greenstone belt, Zimbabwe: Implications for provenance and source region weathering. *Geoch. Cosm. Acta.* **60** (10), 1751-1763 (1996).

48. Beaulieu E., Goddéris Y., Donnadieum Y., Labat D., and Roelandt C., High sensitivity of the continental-weathering carbon dioxide sink to future climate change. *Nat. Clim. Change.* **2**, 346-349 (2012).

49. Canadian Food Inspection Agency, Plant Production: fertilizers section Canada Gazette, Part I, Volume 152, Number 49: Regulations Amending the Fertilizers Regulations

50. de Silva E.F.D., Ammar M., Celso G., Fernando N., Abdelkrim C., Cristina S., Valdemar E., Ana R., Marques F., *J. Hazard. Mater.* **182,** 232–245 (2010).

51. Batarseh M., El-Hasan T., Toxic element levels in the phosphate deposits of central Jordan, Soil and Sediment Contamination: *An International Journal* **18** (2), 205–215 (2009).

52. European Commission (EC), Council Directive (86/278/EEC) on the protection of the environment, and in particular of soil, when sewage sludge is used in agriculture, Official J. European Community, L181 (Annex 1A), p. 6–12 (1986).